Rheological Properties of Gels Formed at the Oil/Water Interface by Reaction Between Tetrameric Acid and Calcium Ion under Flow Condition and at the Batch Scale

Sébastien SIMON*, Estefania BLANCO, Bicheng GAO, Johan SJÖBLOM

Ugelstad Laboratory, Department of Chemical Engineering, the Norwegian University of Science and Technology (NTNU), N-7491 Trondheim, Norway

Nicolas PASSADE-BOUPAT
TOTAL S.A., PERL - Pôle D'Etudes et de Recherche de Lacq, 64170 Lacq, France

Thierry PALERMO, Marianna RONDON-GONZALEZ
TOTAL S.A., CSTJF - Centre Scientifique et Technique Jean Féger, 64018 Pau, France

Abstract

The interfacial reaction between ARN tetrameric acid and Ca^{2+} which leads to the formation of calcium naphthenate deposits was studied using a co-axial capillary device fitted to a profile analysis tensiometer. This device allows to continuously exchange the oil droplet subphase by a fresh ARN containing solution, thus mimicking the flow of oil as in an industrial separator.

The effect of pH was first studied, and it was found there was a formation of a crosslinking structure by reaction between ARN and Ca^{2+} at pH comprised between 7 and 8. Then, the mechanism of growth of the interfacial gel was studied by determining the influence, on the interfacial shear rheology properties, of the exchange time and the contraction of the volume of the droplet. Two mechanisms can explain interfacial gel growth: formation of multilayers due to the constant input flow of ARN and coalescence between droplets reducing the interfacial area.

Keywords:

Tetrameric acids, ARN, calcium naphthenate deposits, interfacial dilational rheology, coaxial capillary system

* Corresponding author. Tel.: (+47) 48 04 90 31 Fax: (+47) 73 59 40 80

E-mail address: sebastien.simon@chemeng.ntnu.no

1 Introduction: Calcium naphthenate deposition and suggestion of formation mechanism

1.1 ARN and Calcium Naphthenate Deposits

ARN[a] is a special family of naphthenic acids present at low concentrations in petroleum crude oil (from non-detectable to a few tens of ppm). It has been shown that it can form calcium naphthenate deposits by reaction with calcium if the pH of the produced water is high enough[1-3]. These deposits are detrimental for the regularities of crude oil production since they can clog different sections of crude oil productions facilities such as the main separator train, the produced water treatment system, and the sand cleaning system[4]. These deposits have been found in fields present in North Sea, Brazil, West Africa, and China[5-10].

ARN, also known as tetrameric acid or tetraacid, has been discovered in 2004 by a joint study between Statoil and ConocoPhillips[1, 2, 11]. Since then, its presence in oil has been considered as a prerequisite for the formation of calcium naphthenate deposits due to their massive concentration in these deposits (a few tens of percent in weight)[12-14]. ARN is a special type of naphthenic acid which is, schematically, composed of 4 cycloalkyl arms linked to a central points[15-17]. A carboxylic acid function is present at the end of each "arm" (structure presented in figure 1). These carboxylic acid groups can be classically ionized (carboxylates) if the pH is high enough[18, 19].

ARN, due to its peculiar structure, presents unique properties among naphthenic acids. In bulk, ARN forms dimer in model oil solvent (xylene) when protonated and very large aggregates (it has not been possible to determine the exact size) in aqueous solution when ARN is fully ionized[20-23]. ARN is very surface active and adsorbs at the oil-water interface, especially when ionized[11, 24]. In this state, ARN can form a gel at the oil-water interface by reaction with calcium[25-28]. It is thought that this gel forming properties is due to the presence of 4 carboxylate groups per molecule acting as reticulation point after reaction with Ca^{2+} similarly to polymeric gels. Two methods have been implemented to detect and study interfacial ARN gels. First, shear interfacial rheology using either a bi-cone geometry or a Du Noüy ring[26, 28, 29], and second, dilational interfacial rheology[27]. These studies have shown, sometimes by using the model compound BP-10, that a minimum pH is required to form a gel. Moreover, asphaltenes and (mono)naphthenic acids can inhibit the gel formation, the latter by acting as cross-linking termination point agent.

[a] ARN is not an abbreviation. It the name of this family of molecules given by its discoverers Baugh et al.[1]. It means "eagle" in old Norwegian.

1.2 Mechanism of Calcium Naphthenate Deposition

The various works performed in the last 14 years on tetrameric acids (both ARN and its model compound BP-10) allow to suggest a deposition mechanism:

1) The depressurization of crude oil during production induce the release of carbon dioxide and therefore an increase of the pH of the produced water[4, 30].
2) ARN, present in the oil phase, is ionized if the pH of the produced water is high enough[18, 19].
3) ARN start reacting with Ca^{2+} at the oil-water interface to form a gel[26, 28, 29].
4) This gel grows with time. One of the possible growth paths could result from coalescence of ARN/Ca^{2+} gel-covered droplets. As the interfacial area of the merged droplets after coalescence is lower than the two initial droplets, the mass of gel per interfacial area should increase if there is no desorption of gel during coalescence. Another possible path would include the formation of a multi-layer gel by accumulation of ARN at interface that would grow up normal to the interface.
5) The gel continues to grow by entrapping particles and other crude oil components leading to the formation of a solid mass.

This model is consistent with field data and results from experiments performed at the batch scale. The influence of pH is very well known. Deposition happens if a minimum pH is reached (higher than at least around 6). Thermodynamic models allowing to determine the onset of precipitation as a function of Ca^{2+}, pH and ARN concentrations have been proposed[31-33]. They assume the existence of a solubility product K_s defined as:

$$\underline{Ca_2ARN} \leftrightarrow 2Ca^{2+} + ARN^{4-}$$

$$K_s = [ARN^{4-}] \cdot [Ca^{2+}]^2 \qquad (1)$$

These simple thermodynamic models have been compared with data obtained at bench scale using model systems and provide a good fit for the model compound BP-10. These models also predict a decrease of the precipitation pH when the concentration of tetrameric acid increases. This is well captured by experiments in which the solubility limit of BP-10 is measured as a function of pH in oil/water system in presence of calcium. Nevertheless, a correction to the equations had to be introduced for ARN[31].

As the concentration of ARN in the oil phase is much lower than in the deposit (a few ppm in weight[34, 35] vs. a few tens of percent in weight), gel formation at interface is a reasonable explanation for the accumulation of ARN in deposit. During oil production, there is a continuous flow of oil and water[36] and therefore ARN continuously adsorb and react with Ca^{2+} allowing the growth of the interfacial gel. In addition, w/o emulsions are generally present in oil production facilities. These emulsions display a large interfacial area. Their coalescence could play a role in the growth of the interfacial gel as the total interfacial area would vary.

1.3 Goal of the Study

This study is a continuation of the work by Subramanian et al.[27] who studied the ARN/Ca^{2+} gel formation, thought to be the starting point in the formation of calcium napthenate deposits (point 3 in the proposed mechanism), by interfacial dilational rheology using a sessile/pendant drop tensiometer. They created a drop containing a solution of ARN in xylene that was suspended in a solution containing NaCl, buffer, calcium chloride at pH=8. They determined interfacial tension and interfacial dilational moduli E' and E'' as a function of ARN concentration, and in presence of crude oil indigenous components.

The goal of this new article is to study different aspects of the mechanism of calcium naphthenate deposition, namely the influence of pH on the gel formation (points 2 and 3) as well as the determination of how the gel growth with time (point 4). These studies are performed using experimental procedures designed to be closer to real operational conditions compared with Subramanian et al.. In particular:

-Experiments were performed using a co-axial capillary device fitted to a profile analysis tensiometer[37-41]. The oil droplet subphase is exchanged by continuous injection of an ARN containing solution in an effort to try to reproduce the continuous flow of oil in petroleum production facility to study the accumulation process of ARN at the oil-water interface.

-The effect of droplet coalescence is modelled with the profile analysis tensiometer by suddenly contracting the oil droplet and following the consequences on interfacial tension and interfacial rheology properties.

-The influence of several parameters (pH, ARN concentration and ionic strength) on gelation has been studied.

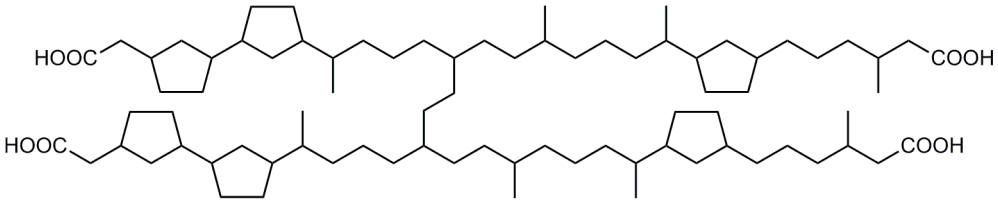

Indigenous naphthenic C_{80} tetraacid

Mw = 1231 g/mol

Figure 1: Formula of the most abundant C_{80} 6-ring tetraacid determined by Lutnaes *et al*. [15, 16]. Redrawn from Lutnaes et al. Republished with permission of Royal Society of Chemistry, from Archaeal C_{80} Isoprenoid Tetraacids Responsible for Naphthenate Deposition in Crude Oil Processing, Lutnaes, B. F.; Brandal, O.; Sjoblom, J.; Krane, J., vol. 4, 2006; permission conveyed through Copyright Clearance Center, Inc.

2 Experimental Section

2.1 Chemicals

The ARN sample has been prepared according to the acid-IER (ion exchange resin) method developed by Statoil[42] from a calcium naphthenate deposits recovered from a North Sea platform. The method has been presented several times (for instance here [12]). Briefly the method consists of the following steps: 1) Cleaning-up the deposit with toluene. 2) Dissolving naphthenate using a 2:1 mass mixture of toluene and 1 M HCl solution. 3) Isolating naphthenic acid by using an ion-exchange resin QAE (strong anion exchanger) Sephadex A-25. 4) Drying up the solid obtained.

The following chemicals were used without further purification: 2-(N-morpholino) ethanesulfonic acid – MES (≥99.5 %, Sigma), 3-(N-morpholino) propanesulfonic acid – MOPS (≥99.5 %, Sigma-Aldrich), sodium tetraborate decahydrate – borax (≥99.5 %, Sigma-Aldrich), sodium chloride (for analysis, Merck), calcium chloride dihydrate (≥99 %, Sigma), xylene (mixture of isomers, ≥98.5 %, VWR). Water was from a Milli-Q system (Millipore).

2.2 Solution Preparations

Solid ARN was dissolved in xylene at a 500 µM concentration and shaken overnight. Then, after filtration (0.2µM PTFE filter), the 500 µM ARN solution was diluted to the required concentration.

Aqueous solutions containing 20 or 600 mM NaCl, 10 mM buffer and 10 mM $CaCl_2$ were prepared and their pH adjusted by adding either 1 M HCl or 1 M NaOH. Different buffers were used: MES for pH=6, MOPS for pH=7, and Borax for all the other pHs.

2.3 Interfacial Dilational Rheology

2.3.1 Apparatus and Principle of Measurements

A sessile/pendant drop tensiometer (PAT 1m - profile analysis tensiometer) from SINTERFACE Technologies (Berlin, Germany) was used in this work. This tensiometer allows to determine the interfacial tension (IFT) by recording the silhouette onto a CCD camera of an oil droplet formed at the tip of a capillary in an aqueous solution using the Young-Laplace equation[43]. For this determination, the densities of the oil and aqueous phase are needed. An accessory for the tensiometer from SINTERFACE Technologies consisting of two concentric capillary tubes (an inner and an outer capillary) was used for the exchange experiments. Every capillary is linked to a 100 µL syringe pump piloted by the SINTERFACE software[37-39, 41]. This co-axial capillary and the procedure are schematically presented in figure 2.

Sessile/pendant drop tensiometer PAT 1m also allows to determine interfacial dilational rheology moduli. The area (A) of a droplet is varied in an oscillatory manner at a given angular frequency (ω) from an initial area (A_0) with an amplitude A_α following equation (2). Concomitantly, interfacial tension varies in a sinusoidal way but with a phase shift[43].

$$\Delta A = A - A_0 = A_a \sin(\omega t) \qquad (2)$$

The complex dynamic apparent dilatational modulus (E*) is defined as the Fourier transform ($\mathcal{F}$) of the change in interfacial tension (γ) relative to the change in interfacial area via equation (3):

$$E^*(\omega) = \frac{\mathcal{F}\{\Delta\gamma(t)\}}{\mathcal{F}\{\Delta\ln(A(t))\}} = E'(\omega) + iE''(\omega) \qquad (3)$$

E* can be split into the real part E', characterizing the elastic properties of the interface and the imaginary part E'', characterizing the viscous properties.

2.3.2 Procedure

In all the procedures the volume of the oil droplet is constantly monitored and controlled by the software.

-The procedure applied to study the influence of pH on the interfacial rheology of the oil-water interface (section 3.1) consists in creating a 15 µL oil droplet composed of ARN solution in xylene using the outer capillary inside a cuvette containing 20 mL of the aqueous phase. Immediately after formation, the oil droplet subphase was exchanged, for 720 s, by injection of the same oil solution through the inner capillary by step of 1 µL every 7 s, equivalent to a flow rate of 0.143 µL/s. In the meantime, the droplet volume was kept constant at 15 µL via feedback control by simultaneously withdrawing oil from the outer capillary. After 720 s, the exchange was stopped. Interfacial rheology measurements started 1200 s after oil droplet formation.

-A similar procedure was implemented to study the influence of exchange time (section 3.2). The difference concerns the exchange times - 3 times were considered (720, 2700, and 5400 s) – and the onset time of interfacial rheology measurements (respectively 1200, 3180, and 5880 s).

-No exchange was performed to study the influence of droplet volume contraction. The volume of the oil droplet containing an ARN solution in xylene was kept constant at 25 µL for 3600 s then the volume was suddenly reduced to 15 µL. This volume was maintained for 900 s before starting the interfacial rheology measurements. This procedure was compared with reference experiments in which the volume was kept constant at 15 µL for 4500 s.

Interfacial dilatational rheology measurements consist of applying five cycles of five different periods (100, 80, 60, 40, and 20 seconds) at a volume amplitude of 3.5% and an average volume of 15 µL. Only the results obtained at a period of 20 s were reported. The interfacial tension response to oscillations were sinusoidal for all the systems considered in the study. Three examples of oscillation responses are presented in the supplementary materials S1. Two typical systems (figures S1.a and S1.b) are shown as well as one of the most “extreme” system i.e. with one of the highest measured E’ (figure S1.c).

Two parallels were at least performed for every system studied. The error bars represent the range of obtained experimental values i.e. the maximum and minimum values obtained.

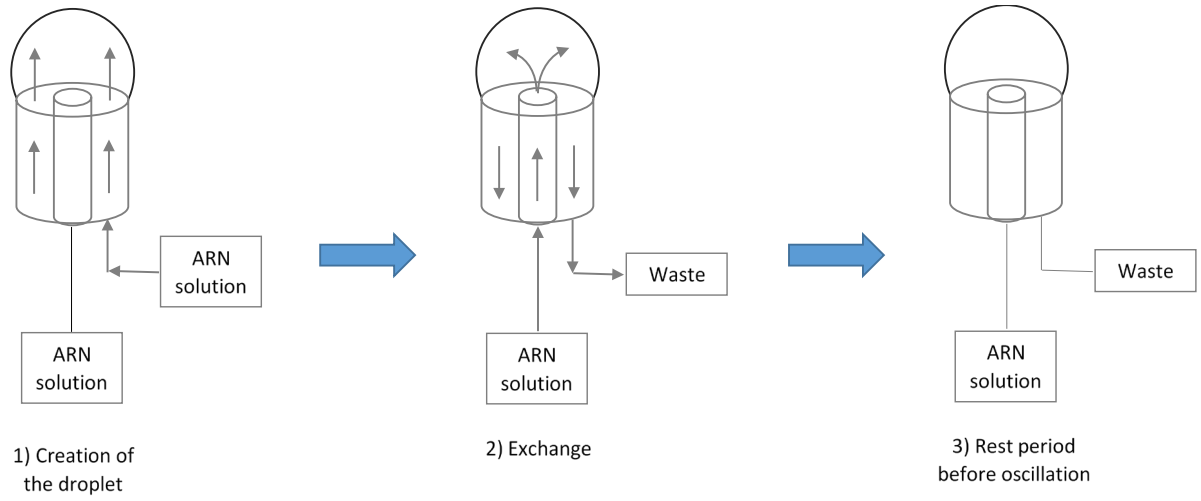

Figure 2: Scheme of the co-axial capillary device and the oil exchange procedure.

2.4 Bottle tests

7.5 mL of aqueous solutions containing 20 mM NaCl, 10 mM buffer and 10 mM $CaCl_2$ and pH adjusted were put into contact with 7.5 mL of ARN solutions in xylene. The mixtures were shaken for 1 hour and then let stand overnight. The next day, pictures of the samples were taken and finally the pH of the aqueous phase (pH_f) were measured.

3 Results

This article is a follow up of the study by Subramanian et al.[27]. they studied the interfacial properties (interfacial tension and interfacial dilational rheology E' and E'') of ARN under carboxylate form at the oil/water interface under quiescent conditions (i.e. no exchange). They found that E' strongly increased (e.g. by a factor of 18 at [ARN]=10 µM) after addition of Ca^{2+} ions in the aqueous phase. This increase was attributed to electrostatic interactions between ARN's COO^- groups and Ca^{2+} leading to the formation of a crosslinked layer at the interface. It is likely the interface is gelled. However, to completely prove the existence of an interfacial gel, the determination of the dynamic mechanical properties, especially at short frequencies, must be performed[44]. Moreover E' and E'' values also depend on several parameters such as adsorption/desorption of surfactant to/from interface. The former are generally modelled by the Lucassen and van den Tempel model[45] assuming that adsorption and desorption are reversible and diffusion-controlled. This model is not valid when gel is formed

at interface and adsorption is irreversible, for instance for some proteins[46]. Consequently, the Lucassen and van den Tempel cannot be applied to the ARN/Ca^{2+} system.

For convenience, tt would be assumed in the present study that a strong value of E' or a strong increase of this modulus would indicate the formation of an interfacial gel even if it has been completely proved as discussed above.

3.1 Influence of pH on the interfacial rheology of the oil-water interface in presence of ARN

3.1.1 Interfacial tension and interfacial rheology results

We have first studied the influence of pH on the ARN/Ca^{2+} interfacial gel formation at two different ionic strengths and ARN concentrations. The aqueous solutions were buffered to prevent any pH variation during the experiments. The kinetic of adsorption of ARN at liquid/liquid interface i.e. variations of interfacial tension with time were determined at different pH under exchange conditions (figure 3). This figure shows there is an evolution of adsorption of ARN at the oil-water interface with pH: Interfacial tension decreases when pH increases then stabilizes between pH 9 and 10, i.e. adsorption increase with the pH due to the ionization of ARN. There also is an evolution of the shape of the interfacial tension variations. At lower pH (6 and 7), the variations of IFT are slow and progressive. However, from pH=8, interfacial tension starts decreasing nearly linearly with time and then suddenly levels off. This sharp transition is different from the usual variations observed for most of the surfactants[47, 48]. This has already been reported for ARN and its model compound BP-10[11, 49] and was attributed to reaction between ARN and Ca^{2+} ions leading to the formation of an interfacial gel. Exchange could also play a role.

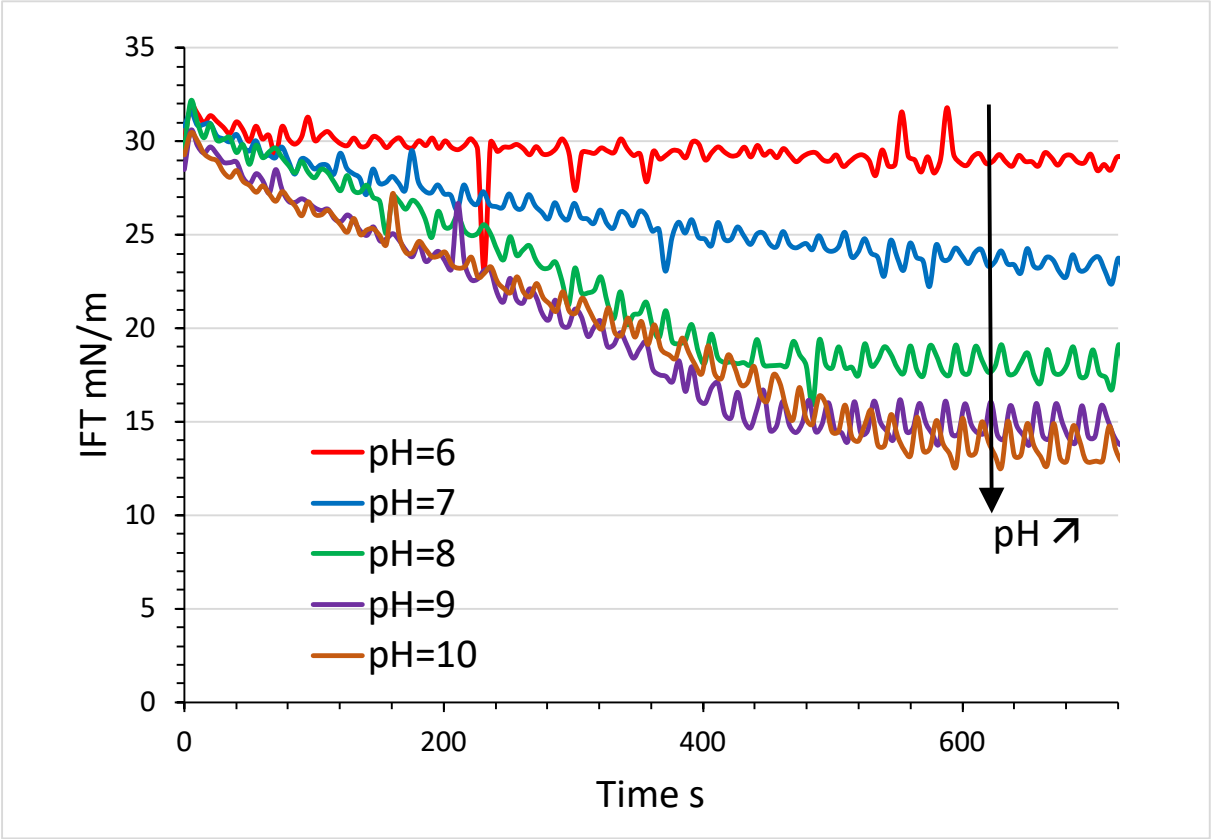

Figure 3: Variations of interfacial tension with time during the ARN exchange period for different pH of the aqueous phase. Conditions: [ARN]= 2.5 µM, [NaCl]=20 mM, 720 seconds of exchange.

480 seconds after stopping the exchange, oscillations were performed to determine the interfacial rheology moduli E' and E'' (figure 4.a). Values of interfacial tension measured at the end of the exchange period (720 s) are also indicated. This figure shows that E' is systematically higher than E'' at all the pHs, indicating a predominantly elastic interface. Moreover, E' increases with pH. At lower pHs (6 and 7), E' values are relatively low and comparable to values obtained for ARN in absence of calcium[27]. There is then a steep increase of E' to values close to 40 mN/m when pH is increased from 7 to 8. Finally, E' levels off at higher pHs. The high E' value from pH=8 seems to indicate that there is formation of an interfacial gel between pH 7 and 8. However, a modification of interface composition happens between pH=6 and 7 since interfacial tension decreases. This could be a sign of ARN ionization onset.

Similar measurements were done by varying the ARN concentration and the ionic strength. Figure 4.c presents the variations of E', E'', and interfacial tension with pH for an ARN concentration of 7.5 µM at the same NaCl concentration (variations of IFT with time at 7.5 µM are presented in supplementary materials S2). Even if the moduli were not measured at pH=9 and 10, similar conclusion can be drawn i.e. there a transition indicating the creation of an interfacial gel between pH 7 and 8. This transition is even more pronounced than at lower concentration since E' increases from 39 mN/m at 2.5 µM to 116 mN/m at 7.5 µM. The gel formation pH is similar for the two tested concentrations because the difference is probably too small to be detected for the pH variation intervals used in the experiments.

Figures 4.b and 4.d presents results obtained for a higher ionic strength ([NaCl]=600 mM) and at ARN concentrations of respectively 2.5 and 7.5 µM. They present a similar transition between pH 7 to 8 as at lower ionic strength. However, the interfacial modulus E' is lower at 600 mM NaCl indicating a weaker structure or an increase of diffusion-exchange processes from and to the interface.

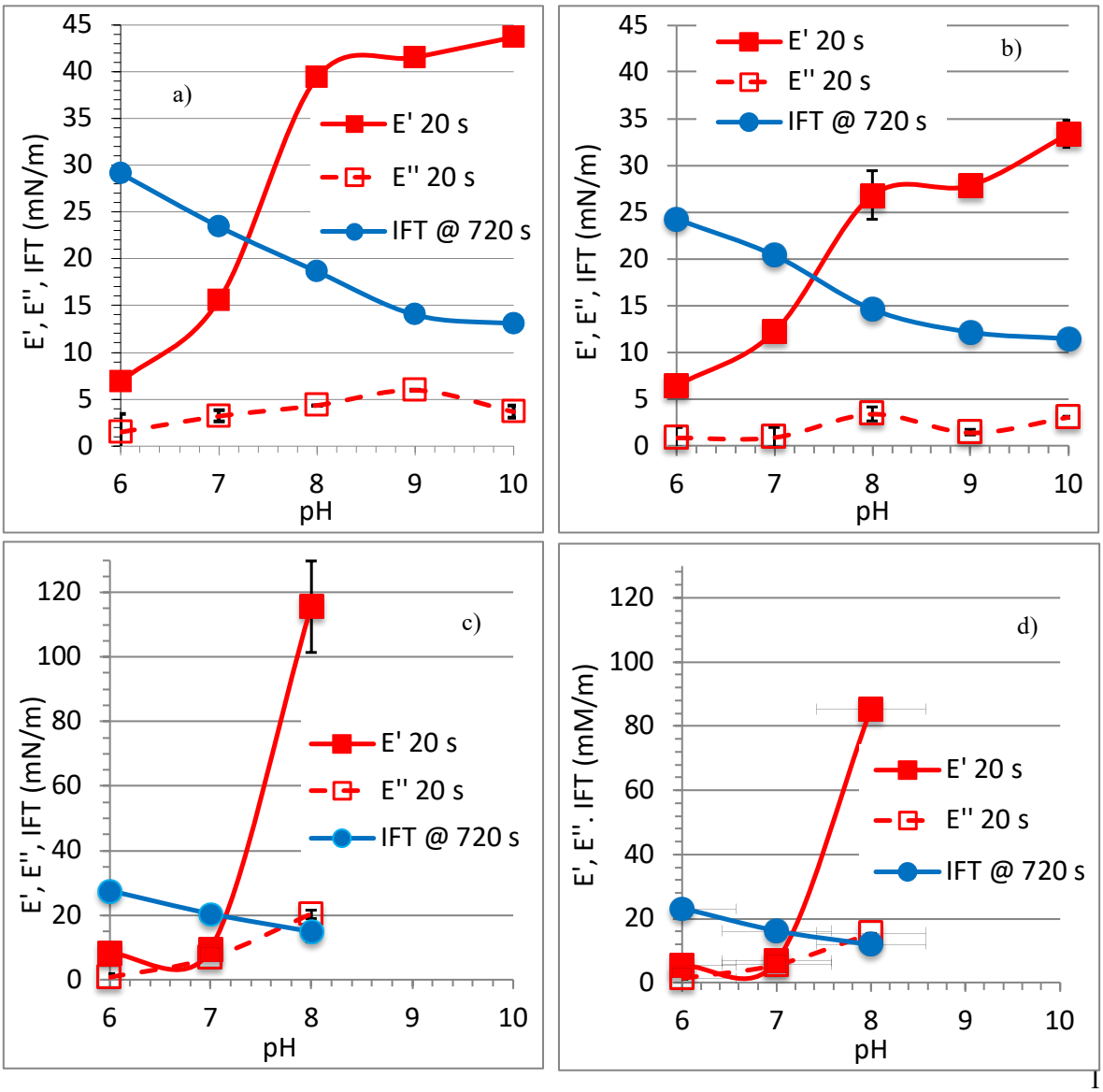

Figure 4: Variations of E', E'' (T=20 seconds), and interfacial tension (measured at the end of exchange period, 720 seconds) as a function of the pH of the aqueous phase. Conditions: a) [ARN]= 2.5 µM, [NaCl]=20 mM, b) [ARN]= 2.5 µM, [NaCl]=600 mM, c) [ARN]= 7.5 µM, [NaCl]=20 mM, and d) [ARN]= 7.5 µM, [NaCl]=600 mM.

3.1.2 Comparison with bottle tests

The interfacial rheology experiments were compared with results obtained by bottle tests. In these tests, an ARN solution in xylene is put into contact with an aqueous solution containing calcium at different pH. After shaking and resting, the aspect of the mixture is visually observed (figures 5 and 6). Visual observation was deemed sufficient to assess the presence or absence of precipitates. The ARN concentration tested (from 57 to 570 µM) are significantly higher than in interfacial rheology experiments to be able to determine if some precipitate are formed. Figures 5.a and 6.a show that a solid is clearly visible at the oil-water interface for samples at pH_f 6.84 and 7.61 (570 µM). This solid is not visible at pH_f=5.99, which means that precipitation starts at a pH comprised between 5.99 and 6.84 for an ARN concentration of 570 µM. The samples at pH_f=8.88 and 9.79 presents a different aspect: the aqueous phase is turbid. A closer examination of this phase by microscopy (figure S3 in supplementary material) seems to reveal that it contains films (mostly likely ARN+Ca^{2+} gels) and droplets.

Bottle tests were also performed at lower ARN concentration (57 µM, figure 5.b, 6.b, and 6.c) and present similar aspects as the samples obtained at an ARN concentration of 570 µM. The main differences lie in the amount of precipitate seen at the interface at $pH_f \approx 6.9$. This precipitate is barely detectable at 57 µM (figure 6.b), which would suggest that the precipitation onset is close to pH=6.9 at this concentration.

The interfacial rheology data presented in section 3.1.1 indicates a gelation happening between pH 7 and 8. However, interfacial dilational rheology experiments were performed at lower concentrations (2.5 and 7.5 µM). As the precipitation onset pH decreases when the ARN concentration increases [31], results obtained by bottle tests and interfacial rheology seem to be consistent indicating a possible match between gelation and precipitation onset. However, a definitive conclusion would require to perform the measurements with both techniques at the

same conditions (ARN concentration, ratio of oil to water volume) which is experimentally difficult. Indeed, a few interfacial rheology tests were performed at ARN concentrations of 15 and 25 µM using the same procedure as in section 3.1.1. While accurate measurements were obtained at pH=6 and 7, the droplet detached from the capillary at pH=8 due to the very low IFT values reached in this condition.

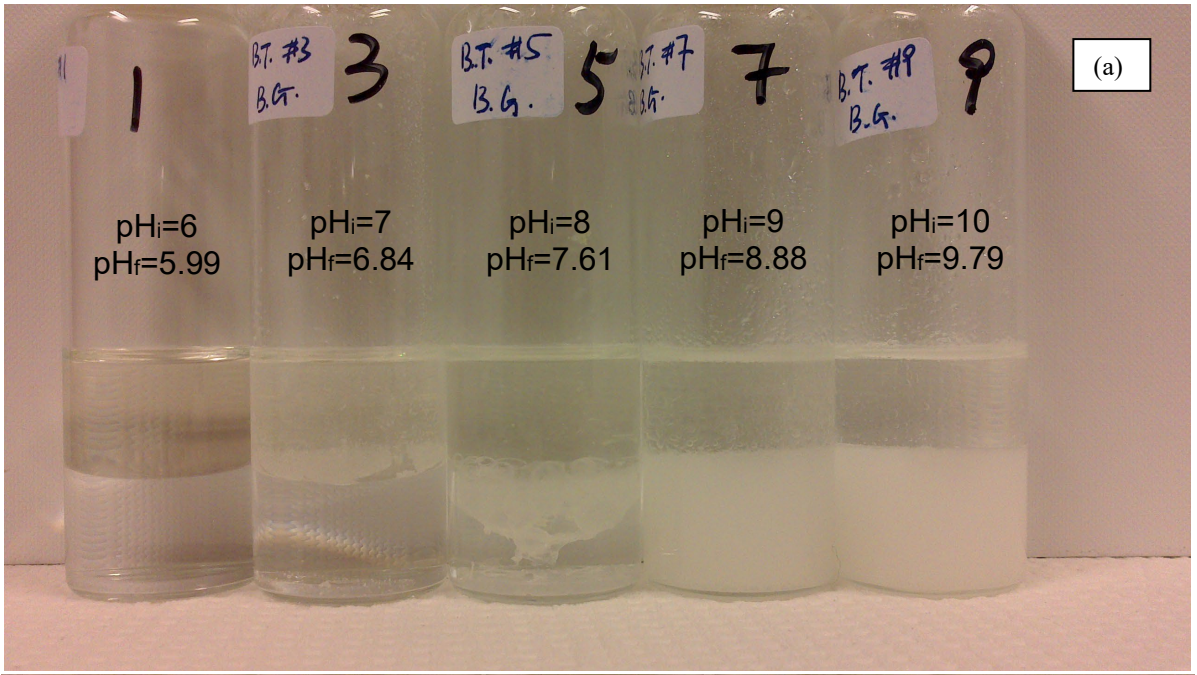

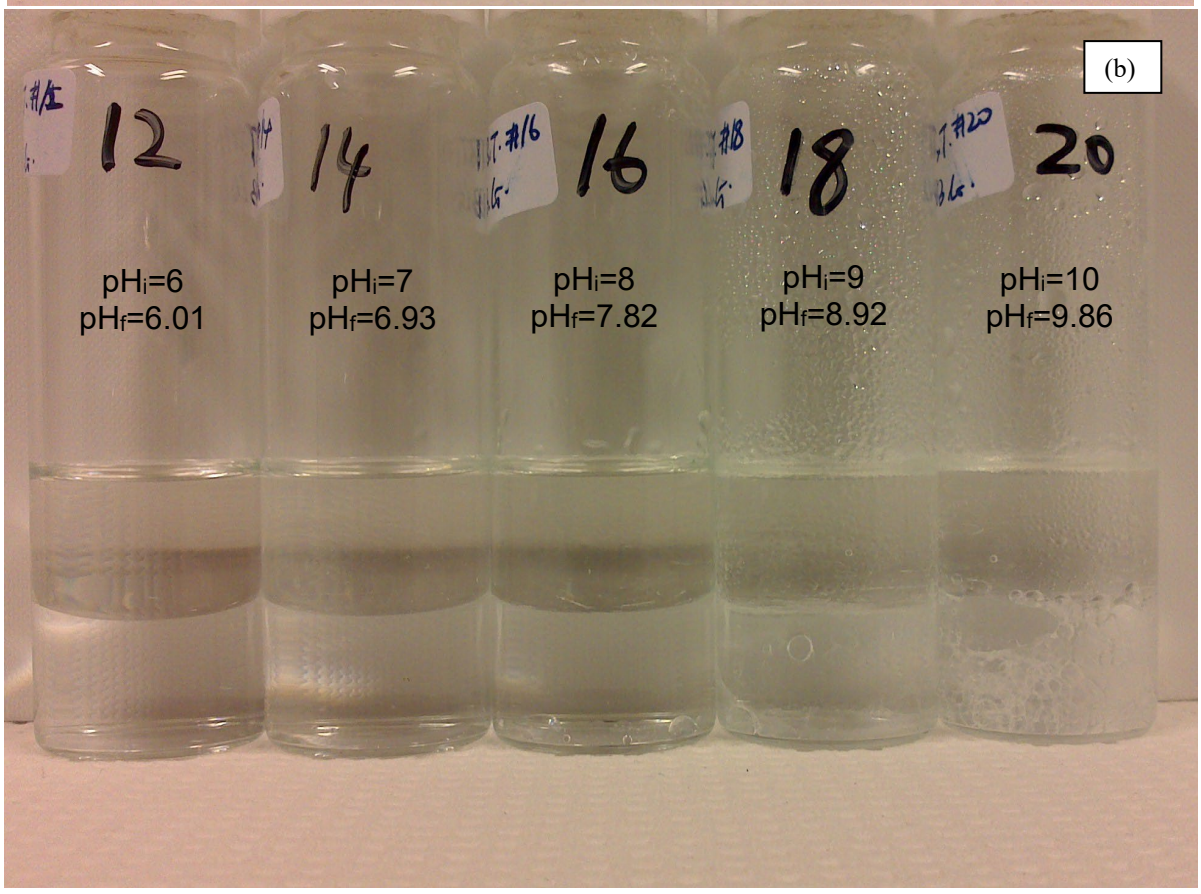

Figure 5: Aspects of mixtures of xylene solutions initially containing ARN and aqueous phases at different pHs after 1 hour of shaking and standing overnight. pH of the aqueous phase were measured before shaking (pH_i) and after standing overnight (pH_f). Reported pH_f values are average from two samples. Conditions: a) [ARN]= 570 µM, and b) [ARN]= 57 µM.

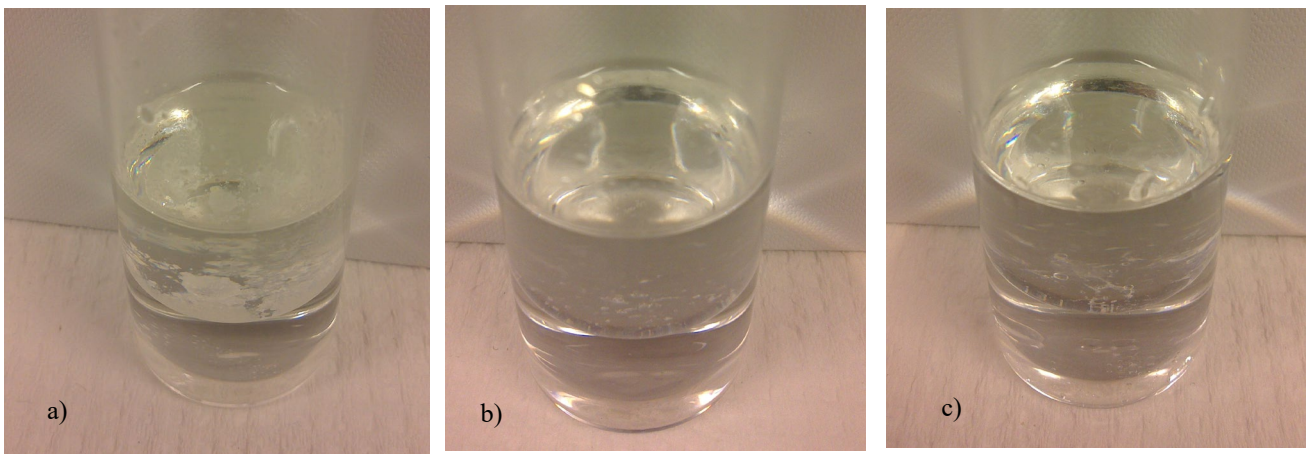

Figure 6: Aspects of mixtures of xylene solutions initially containing ARN and aqueous phases at different pHs and ARN concentration after 1 hour of shaking and standing overnight. pH of the aqueous phase were measured before shaking (pH_i) and after standing overnight (pH_f). Conditions: a) [ARN]= 570 µM, pH_i=7, pH_f=6.84; b) [ARN]= 57 µM, pH_i=7, pH_f=6.93; c) [ARN]= 57 µM, pH_i=8, pH_f=7.82. These pictures need to be compared with figure 5.

3.2 Influence of exchange time

In this section, the accumulation of ARN at interface is investigated. Figure 7 presents the variations of interfacial tension with time while continuously exchanging ARN solution for a long exchange period (90 minutes). The variations are peculiars with a linear decrease of IFT until reaching a first plateau, before decreasing again and reaching a second plateau, and finally decreasing and plateauing off a 3rd time. To the best of our knowledge, we are not aware of other systems presenting similar variations described in the literature. Interfacial rheology moduli E' and E'' were measured after different exchange times (720 seconds, 45 and 90 minutes) (figure 8). It can be clearly seen that E' strongly rises with exchange time going from

36 mN/m to 234 mN/m when exchange times is increased from 720 s to 90 minutes. This clearly indicates the interfacial gel is strengthened with the exchange time. This strengthening as well as the presence of multiple IFT plateaus, indicate there are modifications of the interface due to the constant input flow of ARN. This could mean there is continuous reaction between new arriving ARN and Ca^{2+} present in aqueous phase (Ca^{2+} is in large excess as mentioned in section 4). The IFT plateaus could reflect reorganization or conformation change of ARN/Ca^{2+} at the interface. These plateaus could also reflect the formation of multilayers of ARN/Ca^{2+} indicating a growth of the interfacial gel, even if they should less and less influence the interfacial energy and therefore the interfacial tension values.

The effect of exchange time seems to be partially equivalent to an increase of ARN concentration. Indeed E' increases from 39 to 116 mN/m at pH=8 when ARN varies from 2.5 to 7.5 µM (figures 4.a and 4.c). However, only one IFT plateau is visible during 720 s of exchanges at this concentration (results presented in supplementary materials S2).

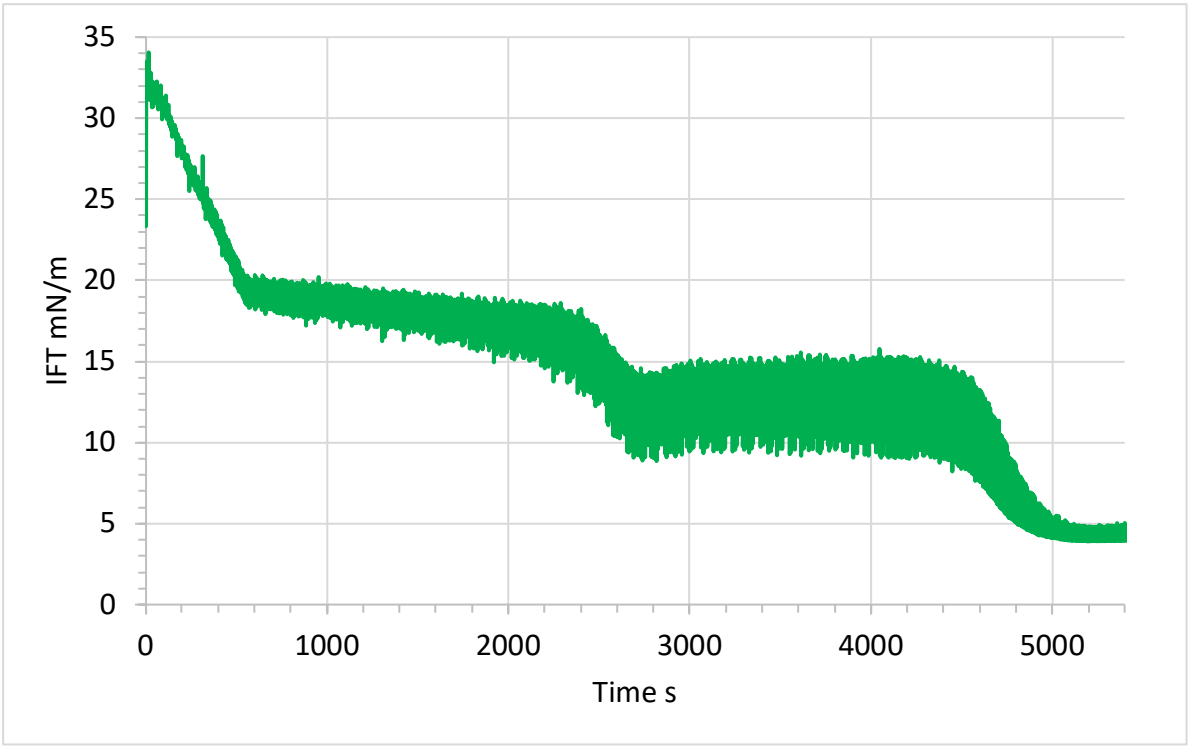

Figure 7: Variations of interfacial tension with time during the continuous exchange of ARN solution inside the droplet (total exchange time=90 minutes). [ARN]= 2.5 µM, [NaCl]=20 mM, pH=8.

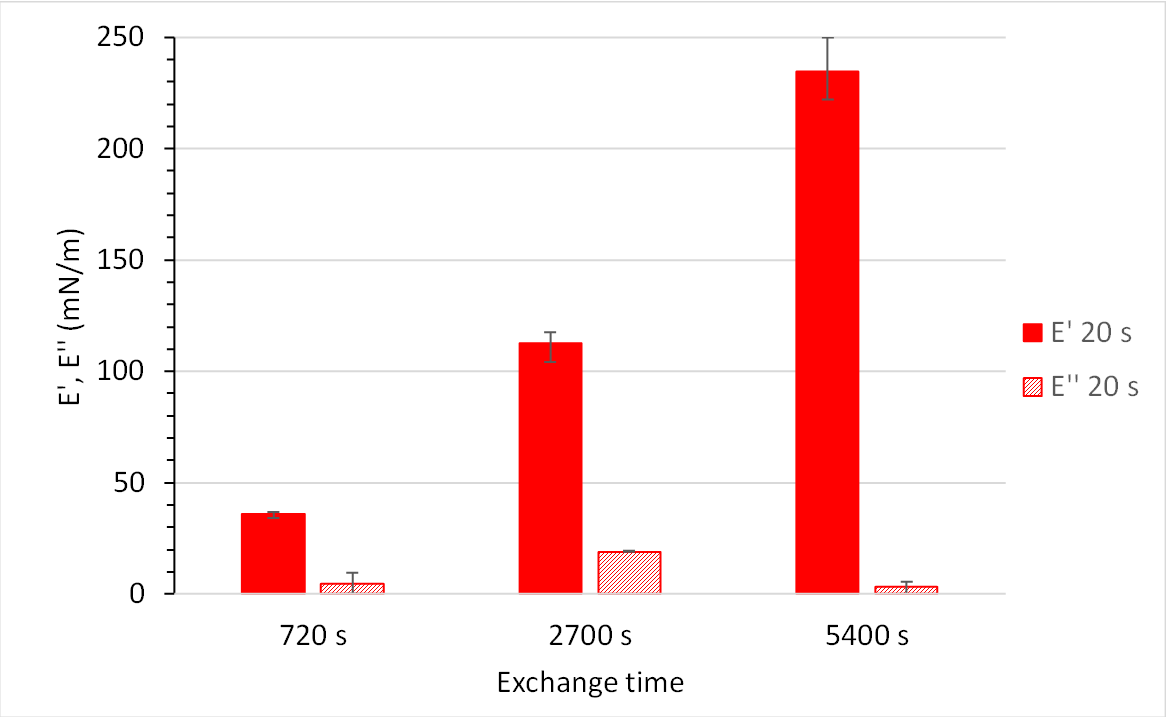

Figure 8: Variations of E', E'' (both measured at a period of 20 seconds) after 720 seconds, 45 minutes, and 90 minutes of exchange of the ARN solution inside the droplet. Conditions: [ARN]=2.5 µM, [NaCl]=20 mM, pH=8. Oscillations after 90 minutes were performed at an amplitude of 3 % (oscillations at 5400 s presented in supplementary materials, S1.c).

3.3 Influence of droplet area contraction

It was mentioned in section 1.2 that droplet coalescence could induce the growth of interfacial gel and accumulation of ARN. Indeed, when two droplets coalesce, the surface area of the new droplets is lower than the sum of the areas of the two initial droplets. Consequently, if the ARN/Ca^{2+} interfacial material does not desorb during the coalescence process, as the adsorbed mass would stay constant and the area would decrease, the adsorbed amount of ARN per surface unit should increase. As a result, ARN/Ca^{2+} interfacial material would accumulate at the interface, and this is therefore a possible mechanism to explain the growth of the interfacial gel. In order to test this mechanism, the volume of the droplet is suddenly contracted (from 25 to 15 µL) and so is the interfacial area, after letting ARN adsorb and react with calcium for 1 hour. This contraction would mimic the reduction of interfacial area during the coalescence process. The interfacial rheology properties of the interface are subsequently determined.

Figures 9 compare the variations of interfacial tension for droplets whose the volume has been contracted after 1 hour of adsorption with reference states consisting of droplets whose volume is constant (15 µL). The value of the volume of the reference state for IFT and moduli values does not seem to be important since similar results were obtained for constant volumes of 15 and 25 µL at ARN concentrations of 5 and 8.5 µM. The small difference of IFT minimum position at 8.5 µM visible in figure 9.b is in the reproducibility range of the experiments. At 2.5 µM, the differences of initial variations of IFT with time between the case where the volume is constant (15 µL) and the case where the volume is contracted after one hour (initial 25 µL) could perhaps come from the difference of initial volume. However, no reference experiment with a constant volume of 25 µL was performed at this concentration to confirm this hypothesis.

Results obtained with an ARN concentration of 2.5 µM (figure 9.a) shows that interfacial tension suddenly decreases after volume contraction and relax back to a value similar to what it was before contraction. The final value after 4500 seconds of adsorption is quite similar to the value measured without volume contraction, which would indicate that the contraction has limited effect on interfacial composition at this concentration.

The situation is different if the ARN concentration is higher (figures 9.b and 9.c). Here, the interfacial tension suddenly decreases after contracting the droplet before slightly increasing and levelling off to a value significantly lower than before contraction or for experiments performed without contraction. This indicates that the interfacial composition has changed after contraction.

The relaxation curves, i.e. the increase of IFT after volume contraction, have been fitted with a double exponential curve to obtain characteristic times of relaxation processes τ_1 and τ_2:

$$IFT = IFT_{3600} + A\left(1 - e^{-t/\tau_1}\right) + B\left(1 - e^{-t/\tau_2}\right) \qquad (4)$$

With IFT_{3600}: IFT right after volume contraction, t: the time elapsed after volume contraction and A and B: fitted parameters. τ_1 and τ_2 are 4 and 95 s (r^2=0.95) at 2.5 µM and 22 and 164 s (r^2=0.996) at 5 µM.

Interfacial rheology moduli E' and E'' for droplets after contraction are compared to the values obtained for droplets whose the volume has been kept constant (figure 10). While E' value is slightly higher for the contracted droplets compared with the droplet whose the volume was held constant at lower ARN concentration (2.5 µM), the modulus E' is much higher for the contracted droplets than for the reference states at 5 and 8.5 µM of ARN. In order to explain these results, we have to consider two limiting cases:

-If the adsorption of ARN is reversible, then the interfacial tension and the E' modulus should be similar to the reference state since the bulk concentrations are similar.

-On the contrary, if ARN does not desorb from interface after volume contraction, then IFT and E' should be respectively lower and higher than the reference state, since the mass of ARN at interface per surface unit is increased due to the reduction of the interfacial area.

Consequently, the decrease of IFT and the strong increase of E' suggest there is accumulation of interfacial material when the interface is reduced and therefore coalescence of droplets allows the interfacial gel to grow and eventually form a deposit.

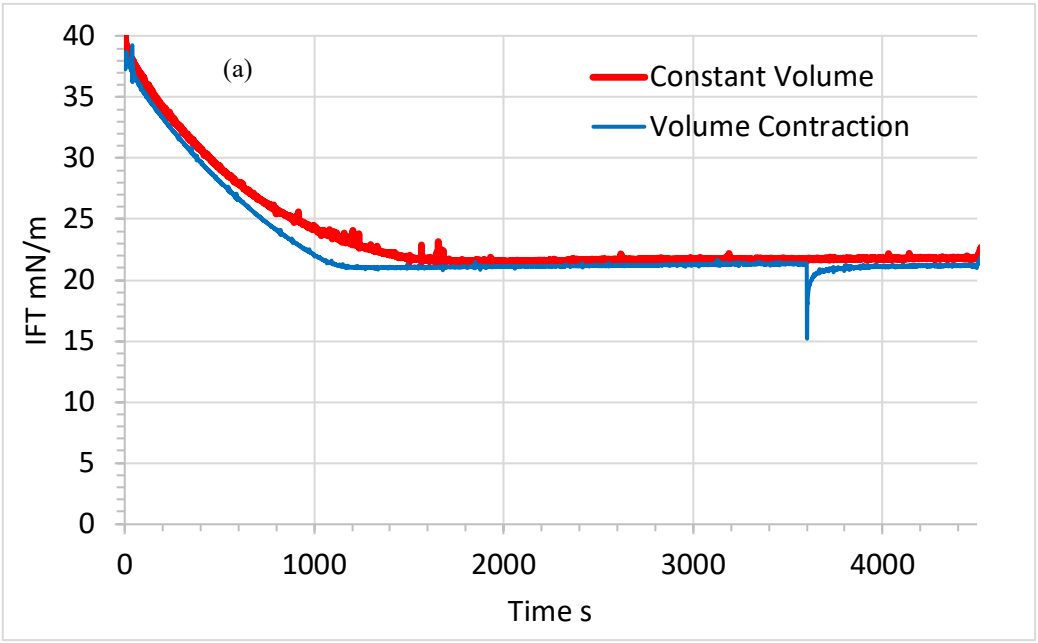

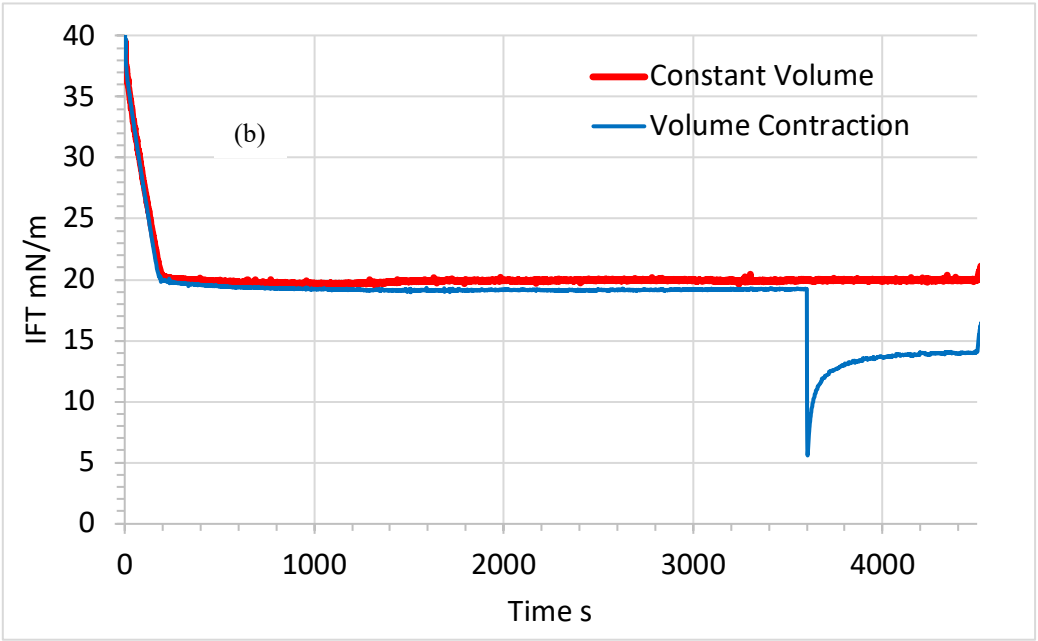

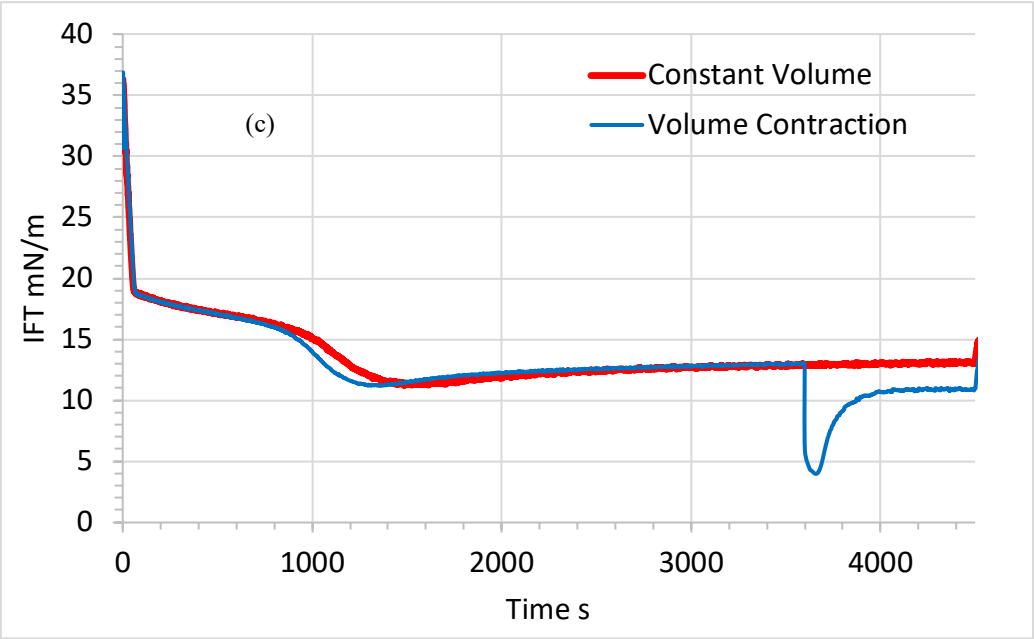

Figure 9: Comparison of the variations of the interfacial tension with time for a droplet whose the volume has been kept constant at 15 µL and another one whose the volume has been contracted from 25 to 15 µL after one hour for a) [ARN]=2.5 µM, b) [ARN]=5 µM, c) [ARN]=8.5 µM. Conditions: [NaCl]=20 mM, pH=8. Figures a) and b) were performed with a hook instead of the co-axial capillary, but similar results were found using the latter.

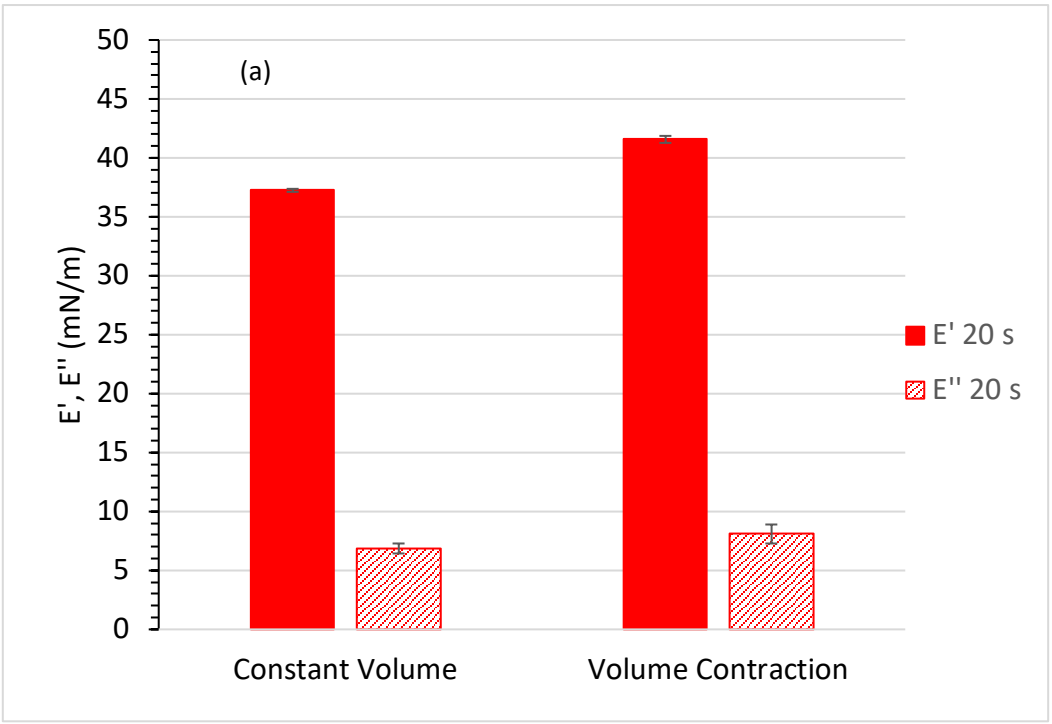

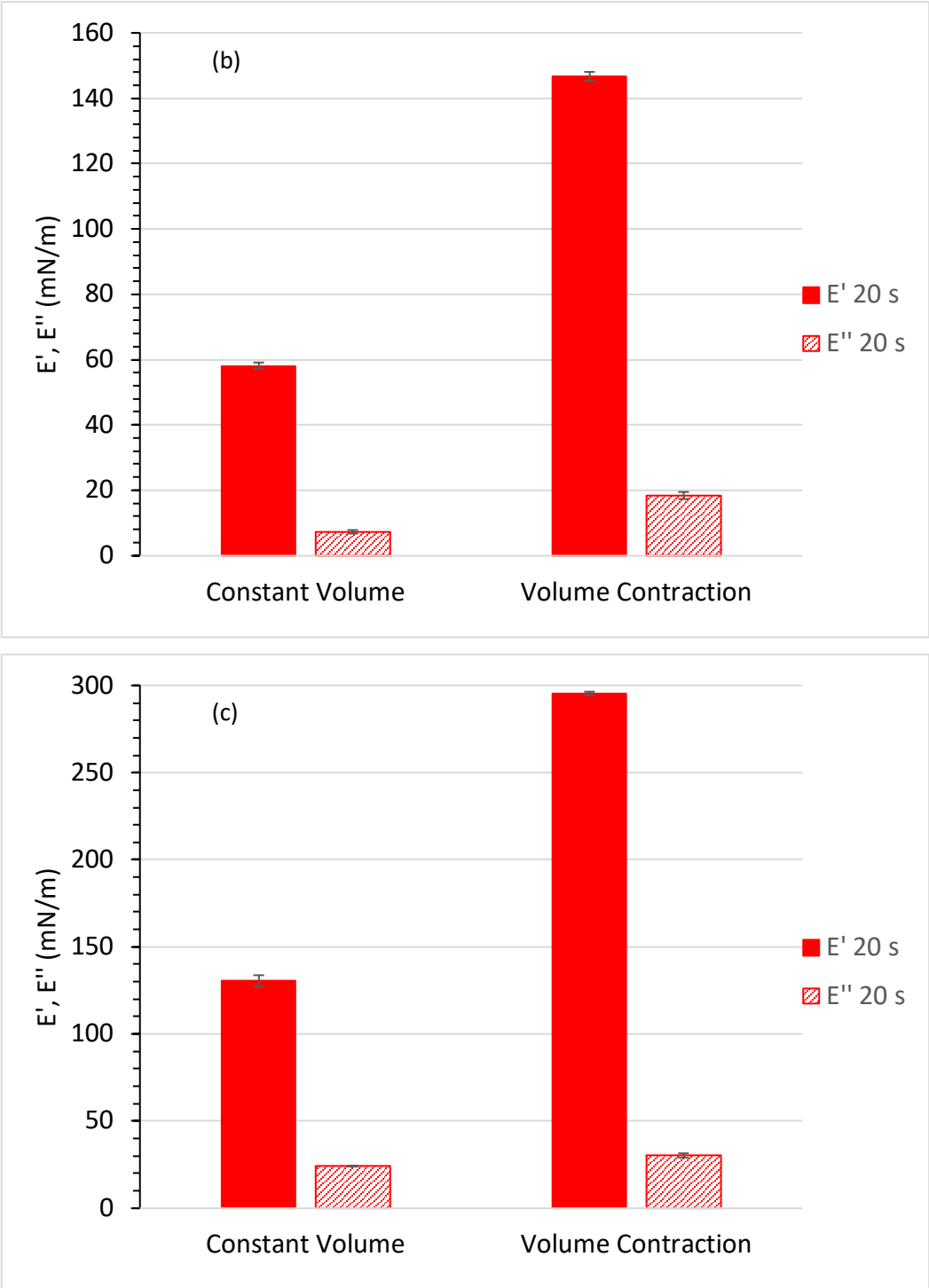

Figure 10: Influence of the droplet volume contraction on E' and E'' (both measured at a period of 20 seconds) for different concentrations of ARN a) [ARN]=2.5 µM, b) [ARN]=5 µM, c) [ARN]=8.5 µM. Left: constant volume of the droplet (15 µL); Right: volume of the droplet=25 µL for 1 hour then contraction to 15 µL. Conditions: [NaCl]=20 mM, pH=8. Figures a) and b) were performed with a hook instead of the co-axial capillary, but similar results were found using the latter.

4 Discussion and Conclusion

The goal of this article was to develop an operational procedure to represent and study several key aspects of the calcium naphthenate deposition at the laboratory scale.

The low concentration of ARN in oil necessarily requires that the tetrameric acid somehow accumulates to form calcium naphthenate deposits. The amount of ARN that would accumulate is brought by the continuous flow of oil in production facilities. The most plausible location for this accumulation is the oil-water interface since:

-Calcium is present in produced water and ARN in oil. The solubility of ARN in water, even fully ionized strongly decreases in presence of NaCl[21].

-ARN is very surface active. This surface activity increases with pH.

-ARN forms an interfacial gel by reaction with calcium.

Consequently, a co-axial capillary device fitted to the profile analysis tensiometer is a suitable device to mimic and study the initial formation of calcium naphthenate deposit. Indeed, it allows to have a continuous flow of ARN solution mimicking the oil phase flow in an industrial oil-water separator while the interface stays still. Nevertheless, there is no continuous flow of the aqueous phase in the exchange experiments performed in this study as there would be in a separator. However, considering the large excess of Ca^{2+} compared to ARN (ratio n_{COOH} from ARN/$n_{Ca^{2+}}$=7.5×10^{-7} to 4.25×10^{-6} mol/mol in Sinterface experiments), there should always be enough Ca^{2+} ions to react with ARN at interface and the absence of aqueous phase flow should not impact the interfacial gelation process.

The interfacial dilational rheology clearly indicates a transition with the formation of an interfacial gel by reaction between ARN and Ca^{2+} between pH 7 and 8. This value is higher than generally reported pH at which the calcium naphthenate starts to deposit[5, 29, 31]. This difference can be explained by the low ARN concentration used in interfacial rheology experiments as well as the very low ratio between the oil and aqueous phase volumes which influences the mass balance.

Two different possible mechanisms for gel growth and ARN accumulation were considered in this article and found plausible: formation of multi-layers of ARN and Ca^{2+} by continuous input flow of ARN and coalescence of droplets.

-Measurements using the co-axial device fitted to the profile analysis tensiometer allowed to test the formation of a multi-layered gel at interface. Interfacial tension variations with time during exchange indicate the presence of several IFT plateaus. These plateaus could indicate either a reorganisation of the interfacial layer or the formation of multi-layers of ARN

and Ca^{2+}. The strong increase of the interfacial modulus E' with time seems to favour the second hypothesis.

-The droplet coalescence mechanism was tested by suddenly contracting droplets and measuring the interfacial moduli after contraction. Results show, if the ARN concentration and most likely the interface coverage is high enough, contraction results in a lower interfacial tension and in a higher E'. ARN is therefore not desorbed and accumulate as multi-layers during coalescence process.

Consequently, the two growth mechanisms appear plausible and could happen simultaneously during oil production. However, other techniques should be implemented such as Langmuir trough's method and ellipsometry to confirm the results and obtain more information.

Co-axial capillary device fitted to a profile analysis tensiometer appears to be a powerful and relevant apparatus to study the formation mechanism of calcium naphthenate deposits. It allows to easily reproduce some key features of this mechanism.

In conclusion, this study has allowed to improve the knowledge of the mechanism of calcium naphthenate deposition. The authors hope this would lead to the development of new prediction and remediation methods of calcium naphthenate deposition.

5 Supporting information:

-Examples of sinusoidal oscillation of drop area and IFT response measured at a period of 20 s.

- Variations of interfacial tension with time during the ARN exchange period for different pH of the aqueous phase. Conditions: [ARN]= 7.5 µM and [NaCl]=20 mM.

-Microscopic picture of a bottle test performed to determine the composition of the turbid bottom phase obtained with the following conditions: [ARN]= 570 µM, pH_i=10, pH_f=9.77.

6 Acknowledgment

The authors thank Total S.A. and Total E&P Norge AS for financial support of the present work and the permission to publish the work. Dr. Vegar Ottesen is acknowledged for performing some control experiments.

7 References

(1) Baugh, T. D.; Grande, K. V.; Mediaas, H.; Vindstad, J. E.; Wolf, N. O. The Discovery of High Molecular Weight Naphthenic Acids (ARN Acid) Responsible for Calcium Naphthenate Deposits, *SPE International Symposium on Oilfield Scale, SPE 93011*, May 11-12 2005; Aberdeen, United Kingdom, 2005.

(2) Baugh, T. D.; Wolf, N. O.; Mediaas, H.; Vindstad, J. E.; Grande, K. Characterization of a Calcium Naphthanate Deposit - The ARN Acid Discovery. *Prepr. - Am. Chem. Soc., Div. Pet. Chem.* **2004,** *49*, 274.

(3) Sjöblom, J.; Simon, S.; Xu, Z. The chemistry of tetrameric acids in petroleum. *Adv. Colloid Interface Sci.* **2014,** *205*, 319.

(4) Vindstad, J. E.; Grande, K. V.; Høvik, K. M.; Kummernes, H.; Mediaas, H. Calcium Naphthenate Management, *8th International Conference on Petroleum Phase Behavior and Fouling*, Pau (France), June 10-14 2007.

(5) Brocart, B.; Bourrel, M.; Hurtevent, C.; Volle, J.-L.; Escoffier, B. ARN-Type Naphthenic Acids in Crudes: Analytical Detection and Physical Properties. *J. Dispersion Sci. Technol.* **2007,** *28*, 331.

(6) Oduola, L.; Igwebueze, C. U.; Smith, O.; Vijn, P.; Shepherd, A. G. Calcium Naphthenate Solid Deposit Identification and Control in Offshore Nigerian Fields *SPE International Symposium on Oilfield Chemistry, SPE 164055*, April 8-10 2013; The Woodlands, Texas, USA 2013.

(7) Vindstad, J. E.; Bye, A. S.; Grande, K. V.; Hustad, B. M.; Hustvedt, N.; Nergård, B. Fighting naphthenate deposition at the Satoil-operated Heidrun field, *SPE 5th International Symposium on Oilfield Scale, SPE 80375*, January 29-30 2003; Aberdeen, United Kingdom, 2003.

(8) Melvin, K. B.; Cummine, C.; Youles, J.; Williams, H.; Graham, G. M.; Dyer, S. Optimising Calcium Naphthenate Control In The Blake Field, *SPE International Oilfield Scale Conference, SPE 114123* May 28-29 2008; Aberdeen, UK, 2008.

(9) Junior, J.; Borges, L. J.; Asomaning, S.; Carmelino, C.; Hango, P.; Milliken, J. D. Calcium Naphthenate Mitigation at Sonangols Gimboa Field, *SPE International Symposium on Oilfield Chemistry*, April 8-10 2013; The Woodlands, Texas, USA, SPE 164069, 2013.

(10) Nichols, D. A.; Rosário, F. F.; Bezerra, M. C. M.; Gorringe, S. E.; Williams, H. L.; Graham, G. M. Calcium Naphthenates in Complex Production Systems - Evaluation and Chemical Inhibition Challenges, SPE-169756 *SPE International Oilfield Scale Conference and Exhibition*, May 14-15; Aberdeen, Scotland 2014.

(11) Brandal, O.; Hanneseth, A.-M. D.; Hemmingsen, P. V.; Sjoblom, J.; Kim, S.; Rodgers, R. P.; Marshall, A. G. Isolation and Characterization of Naphthenic Acids from a Metal Naphthenate Deposit: Molecular Properties at Oil-Water and Air-Water Interfaces. *J. Dispersion Sci. Technol.* **2006,** *27*, 295.

(12) Simon, S.; Nordgård, E.; Bruheim, P.; Sjöblom, J. Determination of C80 Tetra-Acid Content in Calcium Naphthenate Deposits. *J. Chromatogr., A* **2008,** *1200*, 136.

(13) Mapolelo, M. M.; Rodgers, R. P.; Blakney, G. T.; Yen, A. T.; Asomaning, S.; Marshall, A. G. Characterization of naphthenic acids in crude oils and naphthenates by electrospray ionization FT-ICR mass spectrometry. *Int. J. Mass Spectrom.* **2011,** *300*, 149.

(14) Mapolelo, M. M.; Stanford, L. A.; Rodgers, R. P.; Yen, A. T.; Debord, J. D.; Asomaning, S.; Marshall, A. G. Chemical Speciation of Calcium and Sodium Naphthenate Deposits by Electrospray Ionization FT-ICR Mass Spectrometry. *Energy Fuels* **2009,** *23*, 349.

(15) Lutnaes, B. F.; Brandal, O.; Sjoblom, J.; Krane, J. Archaeal C80 Isoprenoid Tetraacids Responsible for Naphthenate Deposition in Crude Oil Processing. *Org. Biomol. Chem.* **2006,** *4*, 616.

(16) Lutnaes, B. F.; Krane, J.; Smith, B. E.; Rowland, S. J. Structure Elucidation of C80, C81 and C82 Isoprenoid Tetraacids Responsible for Naphthenate Deposition in Crude Oil Production. *Org. Biomol. Chem.* **2007,** *5*, 1873.

(17) Smith, B. E.; Sutton, P. A.; Lewis, C. A.; Dunsmore, B.; Fowler, G.; Krane, J.; Lutnaes, B. F.; Brandal, Ø.; Sjöblom, J.; Rowland, S. J. Analysis of ARN Naphthenic Acids by High Temperature Gas Chromatography and High Performance Liquid Chromatography. *J. Sep. Sci.* **2007,** *30*, 375.

(18) Sundman, O.; Nordgård, E. L.; Grimes, B.; Sjöblom, J. Potentiometric Titrations of Five Synthetic Tetraacids as Models for Indigenous C80 Tetraacids. *Langmuir* **2010,** *26*, 1619.

(19) Nordgård, E. L.; Simon, S.; Ahmad, J.; Sjöblom, J. Oil-Water Partitioning for a Synthesized Tetracarboxylic Acid as a Function of pH. *J. Dispersion Sci. Technol.* **2012,** *33*, 871.

(20) Knudsen, K. D.; Simon, S.; Qassym, L.; Gao, B.; Sjöblom, J. Mixed Micelles of Tetrameric Acids and Naphthenic Acids in Water. *Energy Fuels* **2014,** *28*, 4469.

(21) Simon, S.; Knudsen, K. D.; Nordgård, E.; Reisen, C.; Sjöblom, J. Aggregation of tetrameric acids in aqueous media studied by small-angle neutron scattering. *J. Colloid Interface Sci.* **2013,** *394*, 277.

(22) Wei, D.; Orlandi, E.; Barriet, M.; Simon, S.; Sjöblom, J. Aggregation of tetrameric acid in xylene and its interaction with asphaltenes by isothermal titration calorimetry. *J. Therm. Anal. Calorim.* **2015,** *122*, 463.

(23) Kovalchuk, K.; Riccardi, E.; Mehandzhiyski, A.; Grimes, B. A. Aggregates of poly-functional amphiphilic molecules in water and oil phases. *Colloid J.* **2014,** *76*, 564.

(24) Nordgård, E. L.; Magnusson, H.; Hanneseth, A.-M. D.; Sjöblom, J. Model Compounds for C80 Isoprenoid Tetraacids: Part II. Interfacial Reactions, Physicochemical Properties and Comparison with Indigenous Tetraacids. *Colloids Surf., A* **2009,** *340*, 99.

(25) Brandal, Ø. Interfacial (o/w) Properties of Naphthenic Acids and Metal Naphthenates, Naphthenic Acid Characterization and Metal Naphthenate Inhibition. Interfacial (o/w) Properties of Naphthenic Acids and Metal Naphthenates, Naphthenic Acid Characterization and Metal Naphthenate Inhibition, Norwegian University of Science and Technology (NTNU), Trondheim, 2005.

(26) Simon, S.; Subramanian, S.; Gao, B.; Sjöblom, J. Interfacial Shear Rheology of Gels Formed at the Oil/Water Interface by Tetrameric Acid and Calcium Ion: Influence of Tetrameric Acid Structure and Oil Composition. *Ind. Eng. Chem. Res.* **2015,** *54*, 8713.

(27) Subramanian, S.; Simon, S.; Sjöblom, J. Interfacial dilational rheology properties of films formed at the oil/water interface by reaction between tetrameric acid and calcium ion. *J. Dispersion Sci. Technol.* **2017,** *38*, 1110.

(28) Bertelli, J. N.; Dip, R. M. M.; Pires, R. V.; Albuquerque, F. C.; Lucas, E. F. Shear Rheology Using De Noüy Ring To Evaluate Formation and Inhibition of Calcium Naphthenate at the Water/Oil Interface. *Energy Fuels* **2014,** *28*, 1726.

(29) Nordgård, E. L.; Simon, S.; Sjöblom, J. Interfacial Shear Rheology of Calcium Naphthenate at the Oil/Water Interface and the Influence of pH, Calcium and in Presence of a Model Monoacid. *J. Dispersion Sci. Technol.* **2012,** *33*, 1083.

(30) Goldszal, A.; Hurtevent, C.; Rousseau, G. Scale and naphthenate inhibition in deep-offshore fields, *SPE Oilfield scale symposium, SPE 74661*, January 30-31 Aberdeen, United Kingdom, 2002.

(31) Simon, S.; Reisen, C.; Bersås, A.; Sjöblom, J. Reaction Between Tetrameric Acids and Ca2+ in Oil/Water System. *Ind. Eng. Chem. Res.* **2012,** *51*, 5669.

(32) Mohammed, M. A.; Sorbie, K. S. Thermodynamic Modelling of Calcium Naphthenate Formation: Model Predictions and Experimental Results. *Colloids Surf., A* **2010,** *369*, 1.

(33) Mohammed, M. A.; Sorbie, K. S.; Shepherd, A. G. Thermodynamic Modeling of Naphthenate Formation and Related pH Change Experiments. *SPE Prod. Oper.* **2009,** *24*, 466.

(34) Passade-Boupat, N.; Rondon-Gonzalez, M.; Brocart, B.; Hurtevent, C.; Palermo, T. Risk Assessment of Calcium Naphtenates and Separation Mechanisms of Acidic Crude Oil, *SPE International Conference on Oilfield Scale, SPE 155229*, May 30-31 Aberdeen, UK, 2012.

(35) Sutton, P. A.; Rowland, S. J. Determination of the Content of C80 Tetraacids in Petroleum. *Energy Fuels* **2014,** *28*, 5657.

(36) Holt, T.; Olav Jøsang, L.; Sandengen, K. Calcium Naphthenate Propagation during Flow in a Porous Medium. *Energy Fuels* **2013,** *27*, 6440.

(37) Pradilla, D.; Simon, S.; Sjöblom, J. Mixed interfaces of asphaltenes and model demulsifiers part I: Adsorption and desorption of single components. *Colloids and Surfaces A: Physicochemical and Engineering Aspects* **2015,** *466*, 45.

(38) Pradilla, D.; Simon, S.; Sjöblom, J. Mixed Interfaces of Asphaltenes and Model Demulsifiers, Part II: Study of Desorption Mechanisms at Liquid/Liquid Interfaces. *Energy Fuels* **2015,** *29*, 5507.

(39) Ferri, J. K.; Gorevski, N.; Kotsmar, C.; Leser, M. E.; Miller, R. Desorption kinetics of surfactants at fluid interfaces by novel coaxial capillary pendant drop experiments. *Colloids Surf., A* **2008,** *319*, 13.

(40) Ferri, J. K.; Miller, R.; Makievski, A. V. Equilibrium and dynamics of PEO/PPO/PEO penetration into DPPC monolayers. *Colloids Surf., A* **2005,** *261*, 39.

(41) Kotsmár, C.; Grigoriev, D. O.; Makievski, A. V.; Ferri, J. K.; Krägel, J.; Miller, R.; Möhwald, H. Drop profile analysis tensiometry with drop bulk exchange to study the sequential and simultaneous adsorption of a mixed β-casein /C12DMPO system. *Colloid Polym. Sci.* **2008,** *286*, 1071.

(42) Mediaas, H.; Grande, K. V.; Hustad, B. M.; Rasch, A.; Rueslåtten, H. G.; Vindstad, J. E. The Acid-IER Method - a Method for Selective Isolation of Carboxylic Acids from Crude Oils and Other Organic Solvents, *5th International Symposium on Oilfield Scale, SPE 80404*, Aberdeen, United Kingdom, January 29-30 2003.

(43) Derkach, S. R.; Krägel, J.; Miller, R. Methods of measuring rheological properties of interfacial layers (Experimental methods of 2D rheology). *Colloid J.* **2009,** *71*, 1.

(44) Almdal, K.; Dyre, J.; Hvidt, S.; Kramer, O. Towards a phenomenological definition of the term `gel'. *Polym. Gels Networks* **1993,** *1*, 5.

(45) Lucassen, J.; Van Den Tempel, M. Dynamic measurements of dilational properties of a liquid interface. *Chem. Eng. Sci.* **1972,** *27*, 1283.

(46) Kirby, S. M.; Zhang, X.; Russo, P. S.; Anna, S. L.; Walker, L. M. Formation of a Rigid Hydrophobin Film and Disruption by an Anionic Surfactant at an Air/Water Interface. *Langmuir* **2016,** *32*, 5542.

(47) Eastoe, J.; Dalton, J. S. Dynamic surface tension and adsorption mechanisms of surfactants at the air–water interface. *Adv. Colloid Interface Sci.* **2000,** *85*, 103.

(48) Chang, C.-H.; Franses, E. I. Adsorption dynamics of surfactants at the air/water interface: a critical review of mathematical models, data, and mechanisms. *Colloids Surf., A* **1995,** *100*, 1.

(49) Nordgård, E. L.; Sjöblom, J. Model Compounds for Asphaltenes and C80 Isoprenoid Tetraacids. Part I: Synthesis and Interfacial Activities. *J. Dispersion Sci. Technol.* **2008,** *29*, 1114.

For Table of Contents only: